Holzforschung, Vol. 61, pp. 406–413, 2007 • Copyright © by Walter de Gruyter • Berlin • New York. DOI 10.1515/HF.2007.079

# A numerical study of the transverse modulus of wood as a function of grain orientation and properties

**John A. Nairn***

Wood Science & Engineering, Oregon State University, Corvallis, OR, USA

*Corresponding author.
Wood Science & Engineering, Oregon State University, 119 Richardson Hall, Corvallis, OR 97331, USA
Phone: +1-541-7374265, Fax: +1-541-7373385,
E-mail: john.nairn@oregonstate.edu

## Abstract

Finite element analysis was used to study the effective transverse modulus of solid wood for all possible end-grain patterns. The calculations accounted for cylindrical anisotropy of wood within rectangular specimens and explicitly modeled wood as a composite of earlywood and latewood. The effective modulus was significantly reduced by growth ring curvature or off-axis loading, The large changes were attributed to the low transverse shear modulus of wood. The explicit, or heterogeneous, model was compared to prior numerical methods that homogenized properties in the transverse plane. The two models gave similar effective modulus results, but a heterogeneous model was required to capture details in modulus calculations or to realistically model stress concentrations. Various numerical methods for modeling transverse stresses in wood are discussed.

**Keywords:** finite element analysis; grain orientation; numerical modeling; shear coupling; transverse modulus.

## Introduction

Wood within a tree has cylindrical symmetry. Its longitudinal direction is along the tree's axis, while the radial and tangential directions are in the transverse plane. A transverse cross-section of a tree has approximately concentric growth rings. The radial and tangential directions are perpendicular and parallel to these rings. Typical boards are sawn from trees with rectangular cross-sections. A board's axial direction aligns with the tree's longitudinal direction, but its cross-section will have various end-grain patterns, depending on where it was cut from the tree (Figure 1). The various board cross-sections are a consequence of fitting a material with cylindrical symmetry into a shape with rectangular symmetry. This paper describes a numerical study of the transverse properties and stresses for rectangular boards as a function of the end-grain pattern.

Because the longitudinal modulus ($E_L$) of wood is 10–20-fold larger than the radial or tangential modulus ($E_R$ or $E_T$), while $E_R$ and $E_T$ are similar, it is tempting to approximate wood as transversely isotropic. However, in reality, $E_R$ is typically double $E_T$ (Bodig and Jayne 1982); this difference should not be ignored for accurate modeling of transverse stresses. In hardwoods, the stiffer radial direction may be due to ray cells (Price 1929; Schniewind 1959). In softwoods, the stiffer radial direction may be due to alignment of cells in radial rows (Price 1929). Whatever the reason, transverse anisotropy causes some unusual experimental results. Bodig (1963, 1965) observed that $E_R$ of Douglas fir increases as specimen thickness increases. In contrast, Hoffmeyer et al. (2000) found that $E_R$ of Norway spruce decreases as gage length increases. Kennedy (1968) measured transverse modulus as a function of loading angle for several species and found that the modulus varies with angle and can even be lower than both $E_R$ and $E_T$. Shipsha and Berglund (2006) found that $E_R$ of periphery boards far from the pith of Norway spruce is more than double the value for boards close to the pith. These observations are a consequence of the transverse anisotropy of wood and of fitting a cylindrical material into a rectangular specimen. They are also influenced by the particularly low transverse shear modulus, $G_{RT}$, of wood. A low $G_{RT}$ combined with growth ring curvature causes localized deformations that affect modulus experiments (Aicher and Dill-Langer 1996; Aicher et al. 2001; Shipsha and Berglund 2006). Another wood property that may play a role, but is less studied, is the layering of wood into earlywood and latewood material within each growth ring, i.e., the composite structure of solid wood.

A thorough understanding of transverse anisotropy and layering of wood is helpful for analysis of structures and transverse failure modes. For example, variations in end-grain patterns between boards in glulam cause modulus mismatches between layers. These mismatches can induce non-uniform stresses that may promote glue-line failure or transverse tensile failure (Aicher and Dill-Langer 1997; Hoffmeyer et al. 2000). Non-uniform stresses are particularly important for curved glulam subjected to climate changes (Aicher and Dill-Langer 1997; Aicher et al. 1998). Transverse stress analysis is also important for modeling drying cracks or internal checking of radiata pine (Pang et al. 1999; Ball et al. 2001). Since internal checking is confined to earlywood, its analysis requires composite analysis of wood that explicitly accounts for earlywood and latewood properties.

Previous finite element analyses (FEA) of transverse wood properties confirm that transverse anisotropy and low shear modulus are important. Aicher and Dill-Langer (1996) performed FEA of one wide, symmetric board under radial loading and various boundary conditions. Growth ring curvature within the board strongly affected the effective modulus. Hoffmeyer et al. (2000) conducted FEA of glulam with boards loaded in the radial direction and one selected timber structure under tangential loading. The stress concentrations correlated with observed

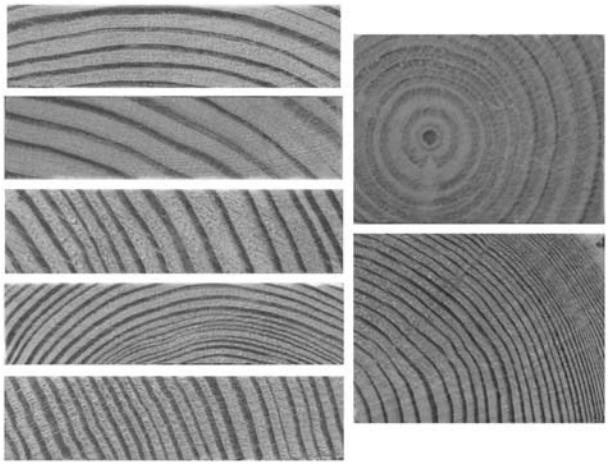

**Figure 1** Sample end grain patterns for rectangular boards cut from a tree with cylindrical structure.

transverse cracks. Aicher et al. (2001) compared experiments to FEA results on a specific board under tangential loading. The experiments confirm the effect of low $G_{RT}$ on transverse wood properties. Jernkvist and Thuvander (2001) used optical methods to measure the radial dependence of mechanical properties. These properties were input to FEA for radial loading of boards of various widths as a function of distance from the pith. Shipsha and Berglund (2006) compared FEA results to radial loading of a board close to the pith and one far from the pith to confirm shear coupling effects in modulus experiments.

Previous numerical studies mostly used homogenized properties in the transverse plane and analyzed only selected loadings or selected board orientations. The purposes of this paper were to explicitly model earlywood and latewood, to compare such heterogeneous calculations to calculations with homogenized transverse properties, and to sample many more end-grain patterns. Various numerical approaches to modeling transverse mechanical properties of wood are discussed.

## Numerical methods

Figure 2 shows one quadrant of an idealized tree with concentric growth rings of earlywood and latewood. All potential cross-sections for rectangular lumber can be sampled from this quadrant by selecting the board centroid, ($x_c$, $y_c$), while maintaining board width and height in the *x*- and *y*-directions. Boards selected this way were analyzed by 2D plane-strain FEA. The FEA mesh was created by partitioning a board's entire cross-section into a square grid of 8-node isoparametric elements. All elements used orthotropic material properties with the tangential, radial, and longitudinal properties initially in the *x*-, *y*-, and *z*-directions. To account for the cylindrical anisotropy of wood, each element's material axes were rotated clockwise by angle

$$\theta = \frac{\pi}{2} - \arctan\frac{y_c^{(i)}}{x_c^{(i)}}, \tag{1}$$

where ($x_c^{(i)}$, $y_c^{(i)}$) is the centroid of element *i*. To model heterogeneous properties, each element was assigned to either earlywood or latewood properties, depending on the radial position of the element centroid. Defining board orientation by centroid

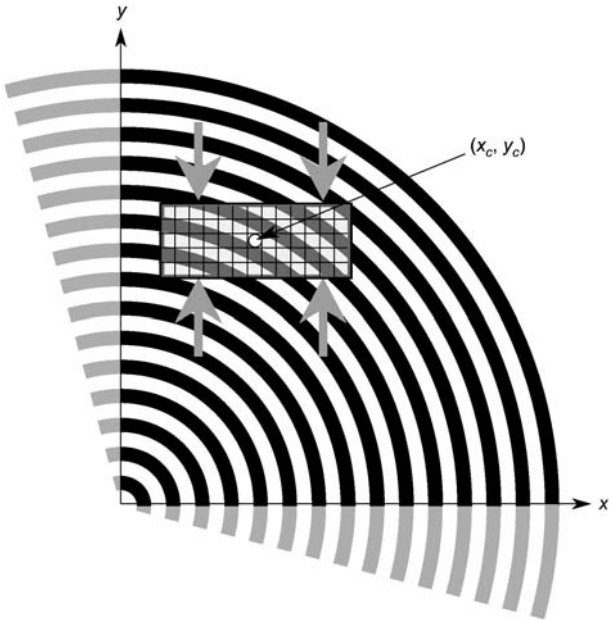


**Figure 2** All possible board orientations can be sampled by orienting the width and height direction along the *x*- and *y*-axes and selecting the board centroid, ($x_c$, $y_c$), from the upper-right quadrant of the *x*-*y* plane. The inset board indicates the FEA mesh was a square grid of elements and loading was in the *y*-direction.

is equivalent to a prior approach based on distance from board bottom to the pith, *d*, and eccentricity, *e*, or distance from board center to a vertical line from the pith (Aicher and Dill-Langer 1996, 1997). The two methods are related by $d = y_c - h/2$ and $e = x_c$, where *h* is board height.

The effective plain-strain transverse modulus was determined by subjecting each board to axial compression in the *y*-direction. Loading was either by uniform displacement or uniform stress conditions. When a board is explicitly heterogeneous (i.e., modeled with earlywood and latewood layers), the stress state is non-uniform and complex. The modulus was thus determined using energy methods. For uniform displacement conditions, the total strain energy, $U_\varepsilon$, can be expressed in terms of an effective modulus, $E_\varepsilon^*$, as (Hashin 1969):

$$U_\varepsilon = \frac{V}{2} E_\varepsilon^* \varepsilon^2, \tag{2}$$

where *V* is the total volume. Thus, the effective modulus is given by:

$$E_\varepsilon^* = \frac{2U_\varepsilon}{V\varepsilon^2}. \tag{3}$$

Similarly, for uniform stress conditions:

$$U_\sigma = V\frac{\sigma^2}{2E_\sigma^*} \quad \text{and} \quad E_\sigma^* = \frac{V\sigma^2}{2U_\sigma}. \tag{4}$$

The two energies, $U_\varepsilon$ and $U_\sigma$, are total strain energies found by FEA.

All simulations were for Douglas fir; typical bulk properties for the longitudinal (L), radial (R), and tangential (T) directions are listed in Table 1 (Bodig and Jayne 1982). To explicitly model earlywood and latewood, their relative fractions and separate properties are required. Growth ring thickness in Douglas fir varies from 2 to 11 mm, depending on location within the tree (larg-

**Table 1** Cylindrically orthotropic material properties for bulk wood, earlywood (EW), and latewood (LW) used in the calculations to model Douglas fir in the longitudinal (L), radial (R), and tangential (T) directions.

| Property | Bulk | EW | LW |
|---|---|---|---|
| $E_T$ (MPa) | 620 | 152 | 1215 |
| $E_R$ (MPa) | 960 | 566 | 1752 |
| $E_L$ (MPa) | 14500 | 10400 | 20700 |
| $G_{RT}$ (MPa) | 80 | 50 | 215 |
| $\nu_{TR}$ | 0.35 | 0.30 | 0.425 |
| $\nu_{TL}$ | 0.033 | 0.033 | 0.033 |
| $\nu_{RL}$ | 0.041 | 0.041 | 0.041 |
| Fraction | – | 0.60 | 0.40 |

No properties are listed for longitudinal shear moduli ($G_{LR}$ and $G_{LT}$) because they have no effect on 2D plain-strain analyses.

er closer to the pith) and on yearly variations in growing rates; the average value is 3.5±2 mm (Taylor et al. 2003; Grotta et al. 2005). X-Ray densitometer measurements show an average latewood fraction of 40% (Abdel-Gadir et al. 1993). All simulations matched these average properties by setting earlywood thickness to 2.1 mm and latewood thickness to 1.4 mm.

There are few experiments on the mechanical properties of earlywood and latewood (Jernkvist and Thuvander 2001), but some qualitative information is available. The earlywood and latewood properties assumed for most calculations are listed in Table 1. These properties were derived as follows.

## Earlywood and latewood properties

**Tangential modulus** Cellular mechanics predicts that transverse moduli scale with density cubed (Gibson et al. 1982; Gibson and Ashby 1997). It was thus assumed that:

$$E_T^{(l)} = E_T^{(e)} \rho^3, \tag{5}$$

where $\rho$ is the ratio of latewood to earlywood density and superscripts (l) and (e) indicate latewood and earlywood properties.

**Radial modulus** This modulus is also a transverse modulus, but recent experiments show that the scaling is less than $\rho^3$ (Modén and Berglund 2007). The reduced scaling is caused by alignment of cells in radial rows, leading to axial deformations that are ignored in cellular theories. Here it was assumed that

$$E_R^{(l)} = E_R^{(e)} \rho^{1.63}, \tag{6}$$

where 1.63 was an arbitrary scaling coefficient between 1 and 3.

**Values for transverse moduli** The above transverse moduli ratios were used in FEA calculations for pure radial loading ($x_c = 0$ and $y_c$ large) and pure tangential loading ($y_c = 0$ and $x_c$ large) and varied until the effective moduli agreed with bulk values for $E_R$ and $E_T$. The density ratio for Douglas fir was set to $\rho = 2$ (Abdel-Gadir et al. 1993). The resulting moduli are given in Table 1.

**Transverse shear modulus** This modulus was found by selecting a reasonable value of $G_{RT}^{(e)}$ and then varying $G_{RT}^{(l)}$ until FEA calculations matched the bulk shear modulus. Pure shear FEA conditions were set by fixing the entire boundary to a pure shear deformation state. A plot of $G_{RT}^{(l)}$ as a function of $G_{RT}^{(e)}$ is given in Figure 3. The results are bounded by a simple rule of mixtures (parallel springs) and an inverse rule of mixtures (series springs), but trends closer to the latter, as often assumed in

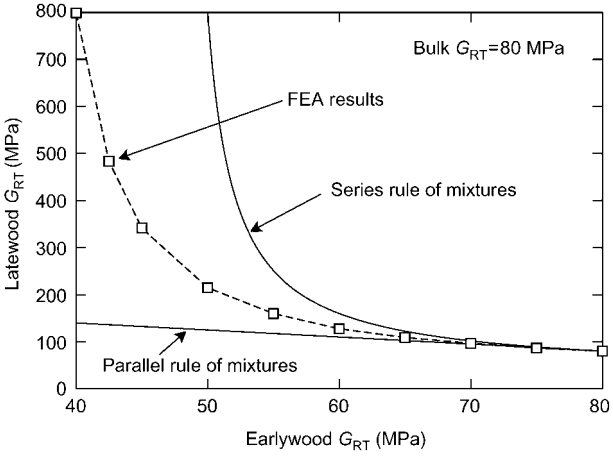


**Figure 3** Latewood shear modulus as a function of earlywood shear modulus when the bulk shear modulus is equal to 80 MPa. The solid lines represent results for calculations of latewood shear modulus using simple composite theories based on springs in parallel or in series.

composite mechanics for shear modulus (Jones 1975). Unless specified, all calculations assumed the specific shear moduli listed in Table 1.

**Transverse Poisson ratio** Optical measurements show that $\nu_{TR}^{(l)} > \nu_{TR}^{(e)}$ (Jernkvist and Thuvander 2001). The values in Table 1 were selected consistent with this finding and such that a rule of mixtures gave the bulk Poisson ratio:

$$\nu_{TR} = 0.35 = V_e \nu_{TR}^{(e)} + V_l \nu_{TR}^{(l)}, \tag{7}$$

where $V_e = 0.6$ is the earlywood fraction and $V_l = 0.4$ is the latewood fraction.

**Longitudinal modulus** Cellular mechanics predicts that longitudinal modulus scales linearly with density (Gibson and Ashby 1997). The values in Table 1 were selected to follow this scaling such that a rule of mixtures gave the bulk longitudinal modulus:

$$E_L = 14{,}500 = V_e E_L^{(e)} + V_l E_L^{(l)}. \tag{8}$$

**Longitudinal Poisson ratios** The longitudinal modulus and Poisson ratios enter plane-strain calculations through plane-strain modifications to the in-plane moduli. For example, the *effective* plain-strain radial modulus is:

$$\frac{1}{E_R^{(\mathrm{eff})}} = \frac{1}{E_R} - \frac{E_L \nu_{RL}^2}{E_R^2}. \tag{9}$$

Since longitudinal properties have only a small effect, the Poisson ratios used were simply the bulk Poisson ratios for both earlywood and latewood.

**Other Poisson ratios** Poisson ratios not listed obeyed the relation:

$$\nu_{ji} = \frac{E_i \nu_{ij}}{E_j}. \tag{10}$$

In summary, the earlywood and latewood properties in Table 1 are not experimental results. They are, however, reasonable values, consistent with known theory and experiments on early-

wood and latewood properties, and consistent with bulk properties.

All calculations were run using the author's FEA software (Nairn 2006). FEA convergence for effective modulus was checked by varying the uniform grid size from 2 mm×2 mm down to 0.25 mm×0.25 mm elements. These calculations found the effective modulus for 10 different board orientations. Element sizes of 0.5 mm×0.5 mm and smaller gave nearly identical results, while larger elements showed minor differences. All subsequent calculations thus used 0.5 mm×0.5 mm elements.

Using a square grid to model curved growth rings can result in rough boundaries between earlywood and latewood, although the roughness is small for fine meshes. To check for numerical problems caused by rough boundaries, some calculations used a modified grid in which nodes near earlywood-latewood boundaries were moved to these boundaries. The differences between a square grid and a modified grid for modulus calculations were negligible. A drawback of the modified grid is that node movement sometimes distorted elements, leading to unrealistic strain calculations. All calculations therefore used the simpler square grid.

## Results and discussion

### Modulus as a function of board orientation

To probe all board orientations, the quadrant in Figure 2 was partitioned into a grid extending from 0 to 500 mm in each direction with grid points separated by 25 mm. FEA calculations were run for 50 mm×20 mm boards located at each of the 441 grid points. Each FEA calculation used a 0.5 mm×0.5 mm square grid, resulting in 4000 elements with 12,281 nodes to mesh the entire board. The effective modulus as a function of position, calculated using uniform displacement conditions, is plotted in Figure 4. For radial loading ($x_c = 0$), the modulus was low near the pith, but increased as $y_c$ increased. Far from the pith ($x_c = 0$, $y_c$ large), the modulus approached the bulk $E_R$. The radial loading results are analogous to numerical results reported by Jernkvist and Thuvander (2001) and the experimental and numerical results of Shipsha and Berglund (2006). Pure tangential loading ($y_c = 0$) was similar, except with a smaller increase because the bulk $E_T$ is smaller. For orientations deviating from pure radial or tangential loading, the modulus rapidly decreased. This rapid decrease is a consequence of the low transverse shear modulus (Aicher and Dill-Langer 1996; Aicher et al. 2001; Shipsha and Berglund 2006). A shear effect maximizes near 45°, where a wide trough of minimum stiffness was observed. Common practice for measuring transverse properties of wood is to select small, straight-grained specimens and measure bulk $E_R$ and $E_T$ (ASTM standard D-143). From the FEA grid results, however, the effective transverse modulus was lower than both $E_R$ and $E_T$ for 82% of the orientations.

The grid calculations were repeated for uniform stress instead of uniform displacement conditions. Figure 5 plots the effective modulus for boards at two constant distances from the pith as a function of the angle between a line to the board centroid and the *x*-axis. "Close" boards were 50 mm from the pith, while "periphery" boards where 500 mm from the pith. The moduli by uniform stress or uniform displacement conditions

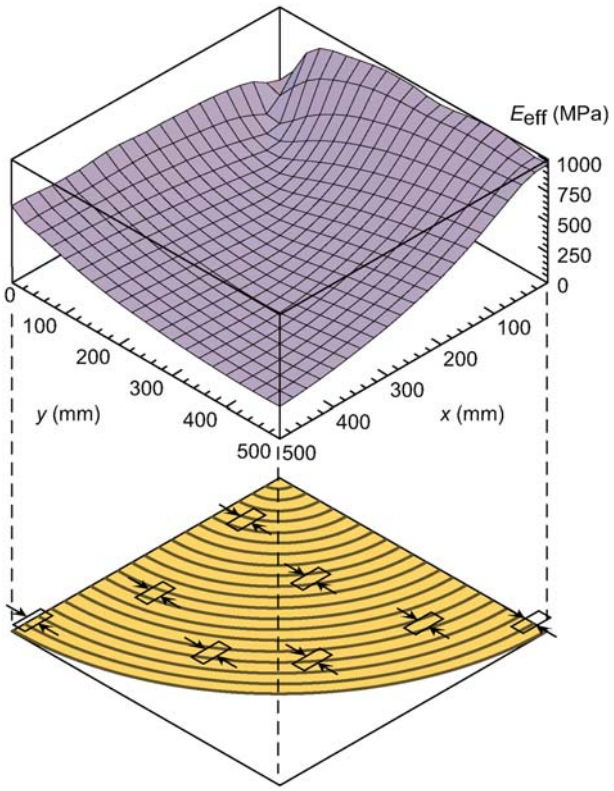


**Figure 4** Effective transverse modulus as a function of board centroid for all possible board orientations. Loading was in the *y*-direction. The boundary conditions were uniform axial displacement.

were similar, although the uniform displacement result was always stiffer. By variational mechanics, a modulus found by imposing displacement boundary conditions and minimizing potential energy (i.e., the FEA process) is a rigorous upper bound to the modulus (Hashin 1969). Although the uniform stress result is not a lower bound (because that would require minimization of complementary energy), it must be lower than the upper bound. Because FEA is converged, however, both results should

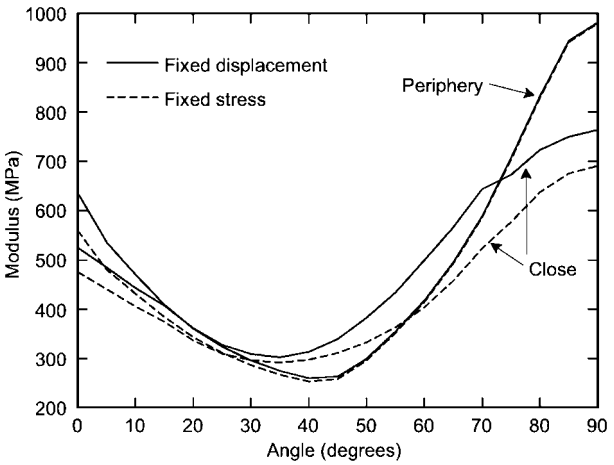


**Figure 5** Effective modulus as a function of angle for "close" boards (centroid 50 mm from the pith) and "periphery" boards (centroid 500 mm from the pith). The solid lines represent results for uniform displacement boundary conditions, while the dashed lines represent results for uniform stress boundary conditions.

be accurate. All subsequent calculations used uniform displacement conditions.

### Heterogeneous calculations vs. homogenized calculations

To study whether layering influences properties, calculations explicitly modeling earlywood and latewood were compared to calculations using homogenized properties (bulk properties in Table 1). Although all elements had the same material properties, each element was still assigned the appropriate angle to model a cylindrically anisotropic material. The modulus for periphery and close boards calculated with homogenized properties (dashed lines) is compared to the heterogeneous model (solid lines) in Figure 6. The similarities show that a homogenized model provided an acceptable approximation for modulus. Differences, however, did arise. For example, the modulus for close boards at low angle was more than 20% stiffer when using homogenized properties. Similarly, the modulus for periphery boards around 15° was more than 15% stiffer with homogenized properties.

Another method to compare homogenized and heterogeneous models is to vary the earlywood and latewood properties while keeping the bulk properties constant. If layering plays a role in mechanical properties, heterogeneous calculations would vary, while homogenized calculations would be constant. Figure 7 shows the modulus of periphery boards for homogenized properties (dashed line) and for heterogeneous calculations with three combinations of shear moduli for earlywood and latewood. The earlywood modulus was set to 40, 50, or 80 MPa, while the latewood modulus was selected to keep the bulk transverse shear modulus equal to 80 MPa. The required latewood shear moduli (from Figure 3) were 800, 215, and 80 MPa, respectively. All models gave the same results at 0°, near 45°, and at 90°, but for other angles, layering influenced the results. The counterintuitive increase in modulus as earlywood shear modulus decreased was because the latewood shear modulus increased more than the earlywood shear modulus decreased. In brief, the layered structure of wood and the relative properties of the layers influence transverse stiffness. A heterogeneous model is required to capture these layering effects.

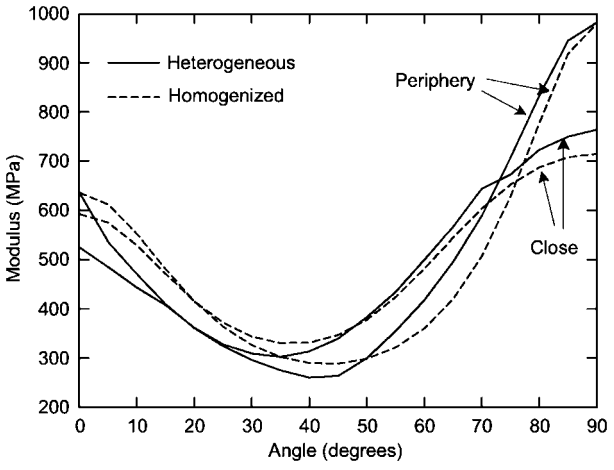


**Figure 6** Effective modulus as a function of angle for "close" boards (centroid 50 mm from the pith) and "periphery" boards (centroid 500 mm from the pith). The solid lines represent results for heterogeneous analysis that explicitly modeled earlywood and latewood, while the dashed lines represent results for homogenized transverse properties.

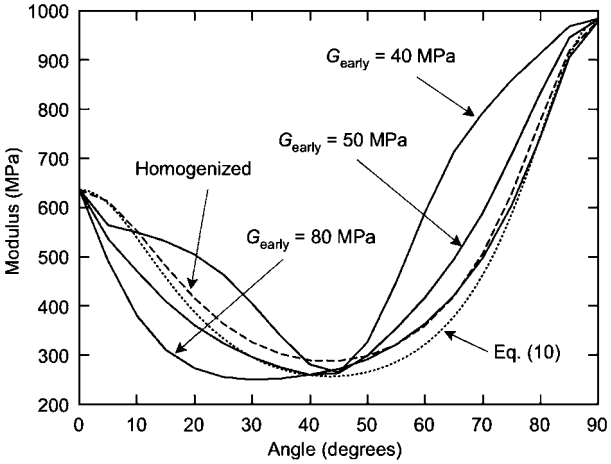


**Figure 7** Effective modulus as a function of angle for "periphery" boards (centroid 500 mm from the pith). The solid lines represent results for heterogeneous analysis and varied earlywood and latewood shear modulus, while keeping the bulk shear modulus constant at 80 MPa. The dashed line represents results for homogenized properties in the transverse plane. The dotted line is the prediction for a rectangularly orthotropic material given by Eq. (11).

One approach to measuring the transverse shear modulus of anisotropic materials is conduct off-axis stress-strain experiments (Price 1929). If a material is rectilinearly anisotropic, rotation of the stiffness matrix gives modulus as a function of angle as (Jones 1975):

$$\frac{1}{E_\theta} = \frac{\cos^4\theta}{E_x} + \left(\frac{1}{G_{xy}} - \frac{2\nu_{xy}}{E_x}\right)\sin^2\theta\cos^2\theta + \frac{\sin^4\theta}{E_y} \qquad (11)$$

This function is plotted in Figure 7 (dotted line). The small differences between Eq. (11) and the homogenized analysis are due to slight growth ring curvature in periphery boards ignored in the equation, but included in the homogenized numerical results. If $E_x$ and $E_y$ are known, measurement of $E_\theta$ can be solved to find $G_{xy}$. Experiments are usually performed at 45°, where the shear effect is greatest and the test would be most sensitive for calculation of $G_{xy}$. The new heterogeneous model results (Figure 7) show that 45° experiments are insensitive to the analysis and thus can measure bulk $G_{RT}$. For any other angle, however, the modulus depends on the relative shear moduli of earlywood and latewood. Perhaps this effect could be exploited to measure earlywood and latewood shear moduli. The suggested experiment is to measure transverse modulus as a function of angle. Results at 0°, 45°, and 90° would measure bulk $E_T$, $G_{RT}$, and $E_R$; results between those angles could be fit using a heterogeneous model to determine earlywood and latewood $G_{RT}$.

The differences between heterogeneous and homogenized analysis are much larger for strain and stress distributions. Figure 8 shows contour plots for strains

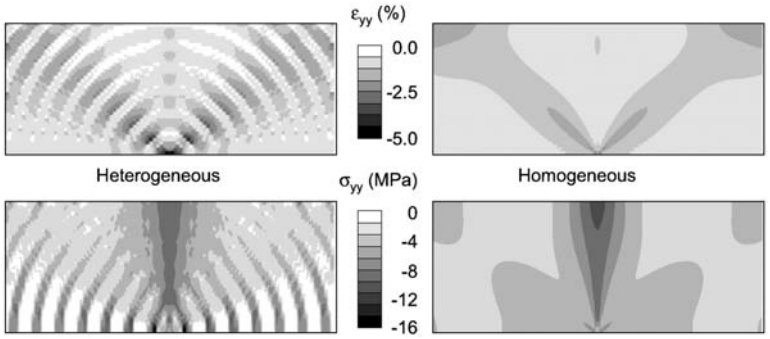


**Figure 8** Contours of *y*-direction normal strain and stress calculated by either heterogeneous or homogeneous analysis. The applied strain was -1.0%. The average stresses were -4.14 MPa for the heterogeneous analysis and -4.40 MPa for the homogeneous analysis.

and stresses in a 50 mm×20 mm board with centroid (0,10), i.e., radial loading for a board with its lower edge at the center of the tree. For the homogenized model (right of Figure 8), the patterns are similar to previous calculations (Shipsha and Berglund 2006). The applied strain was -1%, but the shear effect caused higher strains at 45°; the maximum strain was -2.28%. The average stress was -4.40 MPa, but the maximum stress near the specimen center was -10.9 MPa. The underlying patterns in the heterogeneous model (left of Figure 8) were similar, but the strains and stresses redistribute in earlywood and latewood due to their differing mechanical properties. The redistribution caused greater extremes. The maximum strains occurred in the lower-stiffness earlywood at 45° and reached -4.95%. While the average stress changed only slightly to -4.14 MPa, the maximum stresses occurred in the stiffer latewood at the bottom of the board and reached -15.4 MPa. Thus, when local stress concentrations are crucial for modeling, such as in failure modeling, a heterogeneous model is required to capture these values. A homogenized model may significantly underestimate stress concentrations.

### Effect of board dimensions

Since the effective modulus depends on growth ring curvature across a board, the results depend on board dimensions. To assess dimension effects, calculations were run for 25.4-mm (1.0-in.)-wide boards with thickness varying from 25.4 to 76.2 mm (1.0 to 3.0 in.). These boards were narrower and thicker than in previous calculations. The radial loading results ($x_c=0$) as a function of distance from the pith ($y_c$) are given in Figure 9. For comparison, the previous results for 50 mm×20 mm boards are also plotted (dotted line). Each FEA calculation used a 0.5 mm×0.5 mm square grid and uniform displacement boundary conditions.

Like previous results, the effective modulus for radial loading of narrower boards was lower near the pith, but increased to the bulk radial modulus for periphery boards. Compared to wider boards, the transition to bulk modulus was faster because the edges of narrower boards had less growth ring curvature. These results are similar to previous numerical results for radial loading as a function of width reported by Jernkvist and Thuvander (2001). As the board thickness increased, the difference between pith boards and periphery boards decreased. For boards near the pith (e.g., $y_c=0$), increased thickness includes extra periphery material and thus the effective modulus increased. For boards in the middle (e.g., $y_c=40$ mm), increased thickness includes extra pith material and thus the effective stiffness decreased. For periphery boards, growth ring curvature eventually becomes negligible and the effective modulus approaches the bulk radial modulus.

The board dimensions were selected to match experiments on Douglas fir by Bodig (1963, 1965), for which the radial modulus doubled as the thickness increased from 25.4 mm (1.0 in.) to 76.2 mm (3.0 in.). Unfortunately, Bodig did not specify the distance of the boards from the pith. Although impossible to quantitatively model the experiments, the results in Figure 9 show that doubling of the modulus is possible, depending on board selection. Bodig (1965) claimed the boards were selected with constant $y_c$, although the paper reports no value for $y_c$. Such constant $y_c$ experiments can be predicted by intersections of a vertical line through $y_c$ with the curves for different thickness. Thus, if $y_c$ were 0, the modulus would increase with thickness by 38%. However, if $y_c$ were 40 mm, the modulus would *decrease* by 17%. This latter prediction disagrees with the results of Bodig (1963, 1965), but agrees with more recent results for modulus as a function of gage length by Hoffmeyer et al. (2000).

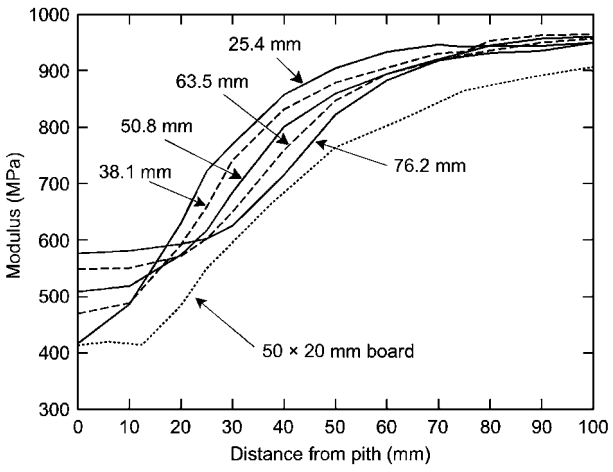


**Figure 9** Effective modulus as a function of distance of the pith for radial loading. The solid and dashed curves are the results for a board of 25.4 mm and various thickness values. The dotted line compares to previous results for a 50 mm×20 mm board.

### Approaches to numerical modeling

Four common methods for numerical modeling of wood are discussed, with emphasis on their suitability for problems involving stress analysis in the transverse plane:

**Transversely isotropic material** The simplest model of wood assumes it is transversely isotropic with the axial direction in the longitudinal direction. The rational is that longitudinal modulus is 10–20-fold larger than radial or tangential moduli, while transverse moduli may differ by less than a factor of two. Approximating transverse properties as isotropic, even if the radial and tangential moduli were identical, is a serious error because it does not allow a low transverse shear modulus, $G_{RT}$, which is important for transverse properties. In an isotropic plane, the shear modulus is typically one-third the tensile moduli (depending on Poisson's ratio), but in wood, $G_{RT}$ is 10–20-fold smaller than the transverse moduli.

**Rectilinear orthotropic material** This model accounts for wood being orthotropic, but simplifies the analysis by aligning coordinates of the anisotropy with the rectilinear global axes, i.e., tangential, radial, and longitudinal directions in *x*-, *y*-, and *z*-directions, or at a constant angle to those directions. This approach simplifies FEA because all elements have the same orientation for their material axes. Because this model can include low shear moduli, it can account for changes in effective modulus due to off-axis loading. The rectilinear assumption, however, makes it only suitable for boards far from the pith. It would completely miss board dimension and orientation effects caused by growth ring curvature within a specimen.

**Homogenized cylindrical orthotropy** This model accounts for growth ring curvature within a specimen, but simplifies the analysis by using homogenized properties in the transverse plane. Compared to rectilinear orthotropy, cylindrical orthotropy complicates the mesh generation. In rectilinear orthotropy, larger elements can be used where stress gradients are small, but in cylindrical orthotropy, small elements are required throughout the specimen to resolve the orientation of material axes along curved growth rings. Homogenized analysis can approximate effective mechanical properties, account for differences between pith and periphery boards, and account for size effects.

**Heterogeneous cylindrical orthotropy** The model used here accounts for both growth ring curvature within a specimen and variations in material properties between earlywood and latewood. This model is physically the closest to approximating the structure of real wood. Although a fine mesh is required to resolve the structure of wood, the extra effort versus homogenized cylindrical orthotropy is minimal. Since the homogenized approach needs a fine mesh to resolve material angle, the only extra work is to additionally assign each element to either earlywood or latewood properties. If earlywood and latewood are particularly thin, the heterogeneous analysis would require an even finer mesh and thus could be more complicated. Differences between homogenized and heterogeneous analyses are discussed above. The most significant differences are the stress concentrations caused by stress and strain partitioning between earlywood and latewood. Heterogeneous analysis is recommended for modeling failure processes induced by localized stresses. The main problem with explicitly modeling earlywood and latewood is obtaining reliable values for their mechanical properties. This paper used reasonable properties. New experimental work to measure their properties would be beneficial.

## Conclusions

Numerical modeling of solid wood under transverse loading was performed for all possible end-grain patterns within rectangular specimens. The effective modulus was strongly affected by loading direction. It was particularly low when the loading direction was neither radial nor tangential over some parts of the board. This off-axis loading effect was due to the low transverse shear modulus of wood. Calculations explicitly modeling earlywood and latewood were compared to calculations using homogenized transverse-plane properties. The results were qualitatively similar for the effective modulus, but significantly different for stress concentrations. Modeling all effects of transverse stresses, particularly when cracking or failure properties are involved, thus requires explicit modeling of the layered structure of wood. Such calculations need more reliable information for the mechanical properties of earlywood and latewood.

## Acknowledgements

This work was supported by the Richardson Family Endowment for Wood Science and Forest Products.

## References

Abdel-Gadir, A.Y., Krahmer, R.L., McKimmy, M.D. (1993) Intra-ring variations in mature Douglas-fir trees from Provenance plantations. Wood Fiber Sci. 25:170–181.

Aicher, S., Dill-Langer, D. (1996) Influence of cylindrical anisotropy of wood and loading conditions on off-axis stiffness and stresses of a board in tension perpendicular to the grain. Otto Graf J. 7:216–242.

Aicher S., Dill-Langer, G. (1997) Climate induced stresses perpendicular to the grain in glulam. Otto Graf J. 8:209–231.

Aicher, S., Dill-Langer, G., Ranta-Maunus, A. (1998) Duration of load effect in tension perpendicular to the grain of glulam in different climates. Holz Roh- Werkst. 56:295–205.

Aicher, S., Dill-Langer, G., Hofflin, L. (2001) Effect of polar anisotropy of wood loaded perpendicular to grain. J. Mater. Civil Eng. 13:2–9.

ASTM standard (2001) D-143, Standard test methods for small clear specimens of timber. Annual Book of ASTM Standards, Volume 4.10 Wood. pp. 25–55.

Ball, R.D., McConchie, M., Cown, D.J. (2001) Heritability of internal checking in *Pinus radiata* — Evidence and preliminary estimates. N.Z. J. For. Sci. 31:78–87.

Bodig, J. (1963) The peculiarity of compression of conifers in radial direction. For. Prod. J. 13:438.

Bodig, J. (1965) The effect of anatomy on the initial stress-strain relationship in transverse compression. For. Prod. J. 15:197–202.

Bodig, J., Jayne, B.A. Mechanics of Wood and Wood Composites. Van Nostrand-Reinhold, New York, 1982.

Gibson, L.J., Ashby, M.F., Schajer, G.S., Robertson, C.I. (1982) The mechanics of two-dimensional cellular materials. Proc. R. Soc. Lond. A 382:25–42.

Gibson, L.J., Ashby, M.F. Cellular Solids: Structure and Properties. Cambridge University Press, Cambridge, UK, 1997.

Grotta, A.T., Leichti, R.L., Gartner, B.L., Johnson, G.R. (2005) Effect of growth ring orientation and placement of earlywood and latewood on MOE and MOR of very-small clear Douglas fir. Wood Fiber Sci. 37:207–212.

Hashin, Z. (1969) Theory of composite materials. In: Mechanics of Composite Materials. Pergamon Press, Oxford. pp. 201–242.

Hoffmeyer, P., Damkilde, L., Pedersen, T.N. (2000) Structural timber and glulam in compression perpendicular to grain. Holz Roh- Werkst. 58:73–80.

Jernkvist, L., Thuvander, F. (2001) Experimental determination of stiffness variation across growth rings in *Picea abies*. Holzforschung 55:309–317.

Jones, R.M. Mechanics of Composite Materials. McGraw-Hill, New York, 1975.

Kennedy, R.W. (1968) Wood in transverse compression. For. Prod. J. 18:36–40.

Modén, C.S., Berglund, L.A. (2007) Elastic deformation mechanisms of softwoods in radial tension – cell wall bending or stretching? Holzforschung, in press.

Nairn, J.A. (2006) Source code and documentation for NairnFEA software and for NairnFEAMPM visualization software. http://oregonstate.edu/~nairnj/.

Pang, S., Orchard, R., McConchie, D. (1999) Tangential shrinkage of *Pinus radiata* earlywood and latewood, and its implication for within-ring internal checking. N.Z. J. For. Sci. 29: 484–491.

Price, A.T. (1929) A mathematical discussion on the structure of wood in relation to its elastic properties. Philos. Trans. R. Soc. Lond. Ser. A 228:1–62.

Schniewind, A.P. (1959) Transverse anisotropy of wood. For. Prod. J. 9:350–359.

Shipsha, A., Berglund, L.A. (2006) Shear coupling effect on stress and strain distributions in wood subjected to transverse compression. Compos. Sci. Technol., in press.

Taylor, A.M., Gartner, B.L., Morrell, J.J. (2003) Co-incident variations in growth rate and heartwood extractive concentration in Douglas-fir. For. Ecol. Manage. 186:257–260.

Received January 18, 2007. Accepted April 13, 2007.